



Published in final edited form as:

Arch Biochem Biophys. 2008 November 1; 479(1): 1–14. doi:10.1016/j.abb.2008.07.026.

LDL PROTEIN NITRATION: IMPLICATION FOR LDL PROTEIN UNFOLDING

Ryan T. Hamilton[§], Liana Asatryan[§], Jon T. Nilsen[§], Jose M. Isas[¶], Timothy K. Gallaher[§], Tatsuya Sawamura[¶], and Tzung K. Hsiai[§]

[§]Department of Pharmacology and Pharmaceutical Sciences, School of Pharmacy, University of Southern California, Los Angeles, CA 90089

^ξDepartment of Biomedical Engineering and Division of Cardiovascular Medicine, Viterbi School of Engineering, University of Southern California, Los Angeles, CA 90089

^ηDepartment of Biochemistry and Molecular Biology, Keck School of Medicine, University of Southern California, Los Angeles, CA 90089

[¶]Department of Pharmaceutical Sciences and Division of Cell Biology, Department of Bioscience, National Cardiovascular Center Research Institute, Osaka University, Japan

Abstract

Oxidatively- or enzymatically-modified low-density lipoprotein (LDL) is intimately involved in the initiation and progression of atherosclerosis. The *in vivo* modified LDL is electro-negative (LDL⁻) and consists of peroxidized lipid and unfolded ApoB-100 protein. This study was aimed at establishing specific protein modifications and conformational changes in LDL⁻ assessed by liquid chromatography/tandem mass spectrometry (LC/MS/MS) and circular dichroism analyses, respectively. The functional significance of these chemical modifications and structural changes were validated with binding and uptake experiments to- and by bovine aortic endothelial cells (BAEC).

The plasma LDL⁻ fraction showed increased nitrotyrosine and lipid peroxide content as well as a greater cysteine oxidation as compared with native- and total LDL. LC/MS/MS analyses of LDL⁻ revealed specific modifications in the apoB-100 moiety, largely involving nitration of tyrosines in the α -helical structures and β_2 sheet as well as cysteine oxidation to cysteic acid in β_1 sheet. Circular dichroism analyses showed that the α -helical content of LDL⁻ was substantially lower (~25%) than that of native LDL (~90%); conversely, LDL⁻ showed greater content of β -sheet and random coil structure, in agreement with unfolding of the protein. These results were mimicked by treatment of LDL subfractions with peroxynitrite (ONOO⁻) or SIN-1: similar amino acid modifications as well as conformational changes (loss of α -helical structure and gain in β -sheet structure) were observed. Both LDL⁻ and ONOO⁻-treated LDL showed a statistically significant increase in binding and uptake to- and by BAEC compared to native LDL. We further found that most binding and uptake in control-LDL was through LDL-R with minimal oxLDL-R-dependent uptake. ONOO⁻-treated LDL was significantly bound and endocytosed by LOX-1, CD36 and SR-A with minimal contribution from LDL-R.

^ξTo whom correspondence should be addressed Tzung K. Hsiai, M.D., Ph.D., Department of Biomedical Engineering and Division of Cardiovascular Medicine, Viterbi School of Engineering, University of Southern California, Los Angeles, CA 90089, USA, Email: hsiai@usc.edu.

Publisher's Disclaimer: This is a PDF file of an unedited manuscript that has been accepted for publication. As a service to our customers we are providing this early version of the manuscript. The manuscript will undergo copyediting, typesetting, and review of the resulting proof before it is published in its final citable form. Please note that during the production process errors may be discovered which could affect the content, and all legal disclaimers that apply to the journal pertain.

It is suggested that lipid peroxidation and protein nitration may account for the mechanisms leading to apoB-100 protein unfolding and consequential increase in modified LDL binding and uptake to and by endothelial cells that is dependent on oxLDL scavenger receptors.

Keywords

LDL; nitration; oxidation; endothelial cells

Introduction

Low density lipoprotein (LDL) particles transport cholesterol, cholesterol esters, lipids, phospholipids, and are involved in the maintenance of membrane fluidity [1]. The LDL particle is comprised of lipid core and an apolipoprotein B-100 (apoB-100) moiety. The latter assumes a pentapartite structure with alternating α -helices and β -pleated sheets (α_1 - β_1 - α_2 - β_2 - α_3) [2]. α_1 anchors the protein to the lipid core; α_2 and α_3 expand and contract across the phospholipid belt of the LDL particle to stabilize electrostatic interactions, thus maintaining LDL protein structural integrity. β -sheets are structurally rigid and engaged in electrostatic interactions with the phospholipids [2].

It is widely recognized that oxidative and/or enzyme-mediated modifications of LDL are required for the particle to acquire the inflammatory properties inherent in the initiation and progression of atherosclerosis [3,4]. This notion is strengthened by the observation that post-translational modifications of apoB100 are elevated in atherosclerotic lesions [5]. Oxidation of LDL can be carried out by transition metals, hemoglobin, myeloperoxidase, ceruloplasmin, and reactive oxygen species generated by vascular endothelium [6–8]. The oxidative modifications render the LDL particle electronegatively charged (LDL⁻) as compared to native LDL (nLDL) [3,9,10]. Also, LDL⁻ (*in vivo* oxidatively-modified LDL) contains elevated level of lipid peroxides and aldehydes that are implicated in protein unfolding [11]. Reactive nitrogen species, especially peroxynitrite (ONOO⁻), generated by the vascular endothelium, nitrate apo-B-100 in LDL particles [10,12–15]. Enzyme-mediated modifications of LDL – accomplished through the action of ubiquitous hydrolytic enzymes– confer atherogenic properties to the lipoprotein particles [4,16]: s-phospholipase A₂ [3] and its free fatty acid product [17], cholesteryl esterases [4], plasmin [18], and matrix metalloproteinase -2 and -9 [18].

This oxidative- and/or enzymatically-modified LDL possesses inflammatory properties: it activates cytokines [19] and monocyte adhesion molecules [20]. The LDL particle is internalized by cells via the ubiquitously expressed LDL receptor (LDL-R). Rather than binding to the LDL-R commonly present in cells, protein unfolding in modified LDL promotes binding to the scavenger receptors (LDL-SR) in vascular endothelial cells [21] and to CD36 in macrophages [11,22]. ONOO⁻-modified LDL is recognized by macrophages, thus gaining further relevance in endothelial dysfunction and initiation of atherosclerosis [15,23,24]. Further, endothelial cells are involved in the initiation of atherosclerosis by the binding of modified LDL and/or apoptotic cells and inducing macrophage/monocyte chemoattractant proteins as well as inducing inflammation [25].

In this study, we assessed specific protein modifications and conformational changes of *in vivo* oxidatively-modified LDL (LDL⁻) and ONOO⁻-treated LDL by liquid chromatography/tandem mass spectrometry (LC/MS/MS) analyses and circular dichroism (CD) spectra. The significance of ONOO⁻-driven modifications is underscored by the implication of both NADPH oxidase (a source of O₂^{•-}) [10,26,27] and eNOS (a source of [•]NO) [28] activities in vascular endothelial dysfunction and by the fast reaction of O₂^{•-} and [•]NO to yield ONOO⁻.

Materials and methods

Chemicals

ONOO⁻ and monoclonal nitrotyrosine antibody were purchased from Upstate Cell Signaling Solutions (UCSS, Lake Placid, NY). Bovine serum albumin, 3-morpholino-sydnonimine (SIN-1), biotin, and 3'-tetramethylindocarbocyanine perchlorate (DiI) were purchased from Sigma (St Louis, MO). Bovine Aortic endothelial cells were purchased from Cell Applications, Inc. (San Diego, CA). Lectin, like oxidized LDL receptor, was a gift from Dr. Tatsuya Sawamura (Osaka University, Japan). CD-36 receptor blocking antibody, SR-A receptor blocking antibody, and LDL-R antibody were obtained from Beckman Coulter (Fullerton, California), Serotec (Raleigh, North Carolina), and Calbiochem (San Diego, California), respectively.

Isolation of *in vivo* LDL and modification of LDL and isolation of LDL⁻

Low density lipoprotein (LDL) was isolated from human plasma (USC blood bank) by density gradient ultra centrifugation and pooled from multiple expired plasma LDL donors as obtained from the USC blood bank (L-80 XP centrifuge, SW-41 rotor, Fullerton CA) [29]. LDL ($\delta = 1.019-1.063$) was then collected and washed with phosphate-buffered saline (PBS) several times using a Millipore (Bedford, MA) centrifugal filtering device with a 30 kDa cut-off. Anion exchange liquid chromatography using a stepwise sodium chloride gradient to isolate nLDL, LDL⁻, and LDL²⁻ to analyze the percentage of LDL⁻. HPLC was performed to analyze the % of LDL⁻. Concentrated LDL (at 200 $\mu\text{g/ml}$) was then incubated with different concentrations of either ONOO⁻ or SIN-1 for 30 min at 37°C. Sin-1 was used as a donor of [•]NO and O₂^{•-} to form ONOO⁻ and to corroborate findings of ONOO⁻-treated LDL [30]. The concentration of ONOO⁻ stock was measured prior to the individual experiments using UV absorption spectra ($\lambda_{302\text{nm}} = 1.67 \text{ mM}^{-1} \text{ cm}^{-1}$) according to the manufacturer's specification (Upstate, Lake Placid, NY).

Analysis of LDL modifications

Oxidation. LDL post-translational modifications were assessed in *in vivo* LDL sub-fractions (LDL) and *in vitro* ONOO⁻/SIN1-treated LDL. Protein oxidation was determined by a decrease in biotin labeling to the oxidized cysteine residues. Biotin labeling was performed by incubating biotin with LDL for 1 h at 37°C to label free unmodified cysteine residues. *Nitrotyrosine*. 2 μg of ONOO⁻-treated LDL and 10 μg of *in vivo* LDL sub-fractions were spotted on Millipore PVDF membranes. 2 μg BSA nitrated with 1 mM ONOO⁻ was used as a positive control. Dithionite was used to reduce nitro groups in the positive control in order to show that the binding was specific. *Dot blot analyses*. Dot blots were performed at a 1:3000 dilution in TBS-Tween for primary nitrotyrosine antibody and 1:10000 dilution for anti-mouse secondary antibody. Similar procedures were performed for 4 μg of biotin-labeled LDL with a monoclonal anti-biotin antibody (dilution at 1:10,000) and a secondary antibody (dilution at 1:10,000), (Sigma, St. Louis, MO). Dot Blots were analyzed using an ECL chemiluminescence kit (Pierce, Rockford, IL), and densitometry was performed using an NIH Scion Image Software (Scion Corp., Frederick, MD) and a product of the density and area determined. The product was also normalized to protein used for both nitrotyrosine and cysteine oxidation analysis. Total nitrotyrosine was quantified by LC/EIS/MS for ONOO⁻-treated LDL samples. Western blot densities for ONOO⁻-treated LDL were plotted against the quantified content of nitrotyrosine in the samples and this standard curve was used to determine the quantity of nitrotyrosine in both the *in vivo* LDL subfractions as well as the SIN-1 treated LDL by extrapolation of the curve. Comparison of nitrotyrosine quantities in the ONOO⁻-treated LDL were comparable to the findings by Leeuwenburgh et al. after normalization to a 1 mg/ml solution [5].

Lipid peroxide measurements

Lipid peroxidation and cholesterol hydroperoxides was measured by the leucomethylene blue assay with *tert*-butyl-hydroperoxide as a standard. LMB cocktail consisted of a 0.05 M pH 5 potassium phosphate buffer with 1.4 g of Triton-X-100 and 5 mg of hemoglobin to 100 ml total volume. 5 mg of LMB was diluted in 8 ml of dimethylformamide and 0.8 ml of LMB dimethylformamide cocktail was added to 10 ml of potassium phosphate buffer. 50 μ g of LDL were incubated with 150 μ l of LMB cocktail for 1 h to a final volume of 200 μ l in 96 well plates. Total tryptophan in apoB-100 was relatively small and any tryptophan hydroperoxides should only be minor contaminants. The colorimetric assay was measured at 650 nm after 1 h incubation at room temperature with a leucomethylene blue cocktail mixture [3]. Molar concentrations of lipid peroxides were determined from a standard curve and total yield of LOOH determined as a ratio of μ moles LOOH/g of LDL protein.

Analysis of specific sites of LDL protein nitration

LDL⁻ and nLDL were isolated from in vivo LDL by HPLC using a stepwise NaCl gradient as previously described [29]. For 100 μ M ONOO⁻-treated LDL, tLDL was analyzed for oxidative modifications. Liquid chromatography tandem mass spectrometry (LC-MS/MS) was performed using a ThermoFinnigan Surveyor MS-Pump with a BioBasic-18 100 mm \times 0.18 mm reverse phase capillary column. The column was equilibrated for 5 min at 1.5 μ L/min with 95% solution A and 95% solution B (A, 0.1% formic acid in water; B, 0.1% formic acid in acetonitrile) and linear gradient was initiated 5 min after sample injection with a ramp to from 95% A to 35% A and 65% B after 50 min and 20% A and 80% B after 60 min. Analysis was obtained by the ThermoFinnigan LCQ Deca XP Plus ion trap mass spectrometer, equipped with a nanospray ion source (ThermoFinnigan) that employed a 4.5 cm metal needle (Hamilton, 950-00954), in a data-dependent acquisition mode. Electrical contact and voltage application to the probe tip were established via the nanoprobe assembly. Spray voltage was set at 2.9 kV and heated capillary temperature at 190°C. Mass spectra were acquired at 400–2000 m/z using a Top 5 method where the five most intense ions for the full scan were subjected to collision induced dissociation, using helium (ms/ms). Peptide identification was achieved using Mascot 1.9 search software (Matrix Science) with confirmatory or complementary analyses by TurboSequest as implemented in the Bioworks Browser 3.2, build 41 (ThermoFinnigan). Spectra were searched against the NCBI human genome database, NCBI build 35. Aromatic nitration and hydroxylation as well cysteine oxidation were assessed using Mascot 1.9 (Matrix Science) for cysteic acid, nitrotyrosine and nitrotryptophan, with confirmatory or complementary analyses that employed TurboSequest as implemented in the Bioworks Browser 3.2, build 41 (ThermoFinnigan) [31,32]. In addition to cysteic acid (+48 Da), nitrotyrosine (+45 Da) and nitrotryptophan (+45 Da), Sequest was used to assess the presence of single or doubly oxidized cysteine (+16 and +32, respectively) as well as tryptophan with both a nitration and oxidation (+61). Quantification of nitrated peptides was carried out by analysis of peak nitration to peak unmodified plus peak modified peptides (NO₂-peptide/ (NO₂-peptide + unmodified peptide). Further positive peptides were analyzed against their y- and b-ions to insure that peptides measured were present and not false positives. They were further analyzed against their peak height to noise ratio.

Circular dichroism spectral analysis of protein structure

Circular dichroism (CD) allows for probing the secondary structure content of proteins. The CD spectrum of modified LDL provides a means to determine the conformational changes of secondary structure in apoB-100 (α -helix, anti-parallel and parallel β -sheet, β -turn, and random coil). In vivo isolated LDL and 100 μ M ONOO⁻-treated LDL subfractions of LDL isolated from HPLC were concentrated and dialyzed to a 0.1 mg/ml solution in chloride free phosphate buffer saline for CD analysis. CD spectra were measured at least ten times to determine the

protein structure. Different secondary structures are represented by the spectrum between 200 and 260 nm. Deconvolution analysis using CD spectra software (CDNN) allowed for assessment of the percent structural integrity in the LDL sub-fractions of modified LDL.

Endothelial cell culture

Bovine aortic endothelial cells (BAEC) between passages 5 and 9 were grown to confluent monolayers in high glucose (4.5 g/l) DMEM (Dulbecco's Modified Eagle's Medium) supplemented with 10% heat-inactivated fetal bovine serum (Gemcell, West Sacramento, CA) and 100 U/ml penicillin-streptomycin (Irvine Scientific, Santa Ana, CA), for 48 h in 5% CO₂ at 37°C.

Binding and uptake of LDL particles

Control and 100 μM ONOO⁻-supplemented LDL particles were treated with 75 mg/ml DiI overnight. DiI-labeled LDL particles were ultracentrifuged, collected, dialyzed, and sterilized to remove the DiI particulate [33]. BAEC were treated with 10 μg/ml DiI-labeled LDL at 0°C for 90 min or at 37°C for 4 h for LDL binding or uptake experiments, respectively [33]. Cells were also treated with 10 μg/ml DiI-labeled LDL with 200 μg/ml of excess unlabeled LDL as a control to exclude DiI labeling of cell membranes and for LDL binding and uptake specificity [33]. Cells were washed thoroughly with DMEM three times after treatment, washed in PBS three times, fixed in paraformaldehyde for 10 min at room temperature, and washed six more times with PBS. Cells were mounted in DAPI-containing mounting medium and visualized using an Axiom 200M Zeiss Fluorescent Microscope (Zeiss, Thornwood, NY) was performed using a DAPI filter for the nucleus and CY3 filter for the DiI-labeled LDL. Quantification of mean intensity and image analysis were assessed by slidebook software (Santa Monica, CA).

Receptor blocking—BAEC were pre-treated for 1 hour with a 1:250 dilution of receptor blocking antibodies to LOX-1, CD36, SR-A, and LDL-R to determine receptor involvement in control- and ONOO⁻-LDL binding and uptake. BAEC were pre-treated with receptor blocking antibodies as follows; (1) no receptor blocking (all active), (2) All receptors blocked (all four inactive), (3) all receptor blocking except LOX-1 (LOX-1 active), (4) all receptor blocking except CD36 (active CD36), (5) all receptor blocking except SR-A (Active SR-A), and (6) all receptor blocking except LDL-R (active LDL-R). Uptake and binding of DiI-labeled control- and ONOO⁻-LDL were performed by the methods described above.

Statistical analysis

Data were expressed as mean ± SD and compared among separate experiments ($n = 3$). For comparisons between two groups, two-sample independent-group t-tests were used (one tail and type 3 t-test analysis). Comparisons of multiple values were made by one-way analysis of variance (ANOVA), and statistical significance among multiple groups determined by the Tukey test (for pair-wise comparisons of means between control and treatments). P -values of < 0.05 are considered statistically significant.

Results

Post-translational modifications of in vivo LDL⁻

In vivo native LDL (nLDL) and LDL⁻ were isolated from total LDL (tLDL) using anion exchange chromatography as described in the Materials and Methods section. The average of LDL⁻ isolated from tLDL *in vivo* was $1.05 \pm 0.05\%$ of the total LDL protein for the purposes of these experiments. LDL nitration was assessed by immunoreactivity to nitrotyrosine antibody (Fig. 1A). While nitrotyrosine was not detectable in either nLDL or tLDL, it was prominent in the LDL⁻ fraction ($n = 3$; $P < 0.001$; Fig. 1A). Oxidation of the 9 free cysteine

residues in the *in vivo* LDL subfractions was assessed by biotin labeling of free cysteine (Fig. 1B). LDL⁻ harbored a significantly lower level of free cysteine in comparison with nLDL and tLDL: nLDL < tLDL < LDL⁻ ($n = 3, P < 0.001$), thus suggesting an elevated amount of cysteine oxidation in LDL⁻ (Fig. 1B). Also worth noting was a 3-fold increase in lipid peroxides in LDL⁻ in comparison with nLDL and tLDL ($n = 3, P < 0.001$) (Fig. 1C).

LC/MS/MS analyses of *in vivo* LDL⁻ revealed specific modifications in the apoB-100 moiety (Table 1): tyrosine (Tyr), tryptophan (Trp), cysteine (Cys), and phenylalanine (Phe) underwent nitration/oxidation in both α helices and β sheets; namely, α_1 (Tyr^{276,666,720}, Trp⁵⁸³), α_2 (Tyr²⁵²³), β_2/α_3 (Phe³⁹⁶⁹), β_1 (Cys¹¹¹²), α_3 (Tyr⁴¹⁴¹), and β_2 (Tyr^{3139,3295,3489}) (Table 1) as corroborated by the Mascot and Sequest scores as well as analysis of peptide and peptide ion masses. These data suggested a large extent of protein modification in the electronegative subfraction or modified LDL subfraction *in vivo* which are consistent with a purification of the *in vivo* oxLDL (LDL⁻). It was further noted that the nitration levels were similar in content to that of 100 μ M ONOO⁻-treated LDL. Cys¹¹¹² in β_1 sheet was oxidized to cysteic acid. Modifications of these peptides are shown in the supplemental (Supplemental, Fig. 1–12) and indicate that spectra are accurate.

Circular dichroism and protein post-translational modifications

Previous studies have suggested that LDL⁻ had significantly unfolded α -helical structure [11,34]. Circular dichroism analysis was used in order to establish an association between specific LDL protein modifications and protein structure [3,11,34]. *In vivo* LDL sub-fractions (Fig. 2A,B) displayed a decrease in optical rotativity at 200–260 nm from LDL⁻ to tLDL to nLDL (Fig. 2A). Increasing optical rotativity at the 220 nm valley reflects a loss in α -helical character and an increase in β -structural components as determined by deconvolution (Fig. 2B). Deconvolution analysis using CD spectra software (CDNN) determined the percent structural integrity of the aforementioned components in LDL sub-fractions of *in vivo* modified LDL. The α -helical content in nLDL (~90%) was largely higher than that in LDL⁻ (~25%), thus suggesting substantial protein unfolding in the latter. These data suggest an association between α -helical nitration (Table 1), lipid peroxidation (Fig. 1C), and protein unfolding (Fig. 2) in LDL⁻.

Characteristics of ONOO⁻-modified LDL

Treatment of LDL with ONOO⁻ induced tyrosine nitration in apoB-100 protein in a dose-dependent manner (Fig. 3A; $n = 3; P < 0.01$). Upon analysis of total mmoles of nitrotyrosine to tyrosine precursor, these data for ONOO⁻-treated LDL were similar to the work by Leeuwenburgh et al. [5]. Densitometry analysis of biotin labeling of free cysteine showed an exponential decrease in the level of free cysteine, thus suggesting increased cysteine oxidation in response to ONOO⁻ treatment ($n = 3, P < 0.001$) (Fig. 3B). Treatment of LDL with ONOO⁻ induced a dose-dependent accumulation of lipid peroxides in LDL (Fig. 3C). HPLC analysis revealed a dose-dependent linear increase in the percentage of LDL⁻ in response to ONOO⁻ treatment (Fig. 3D); this increase was paralleled by an increase in nitrotyrosine- (Fig. 3A) and lipid peroxide (Fig. 3C) content. Oxidized lipid-derived aldehydes were also significantly elevated in response to ONOO⁻ treatment (data not shown). It may be surmised that both lipid peroxides and nitrotyrosine formation are involved in ONOO⁻-induced modification of LDL to an atherogenic form (LDL⁻).

Table 2 lists the nitration and oxidation sites in the apoB-100 protein upon treatment with 100 μ M ONOO⁻: α_1 (Tyr^{103,413,666}), α_2 (Tyr²⁵²⁴), β_2 (Tyr^{3490,3791}), β_2/α_3 (Phe³⁹⁶⁵), and α_3 (Tyr⁴⁰⁸⁸). Neither *in vivo* LDL⁻ (Table 1) nor ONOO⁻-treated LDL (Table 2) showed nitration of β_1 . Similarly to *in vivo* LDL⁻, ONOO⁻ treatment elicited β_2 nitration at Tyr³⁴⁹⁰ (in addition to Tyr³⁷⁹¹). The phenylalanine residue between β_2 and α_3 underwent hydroxylation as also

observed in *in vivo* LDL⁻. These data strengthen the notion that *in vivo* LDL⁻ may originate from ONOO⁻-driven modifications at specific sites in apoB-100 protein. Modifications of the peptides shown above are described in the supplemental (Supplemental, Fig. 13–20).

Circular dichroism analysis of ONOO⁻-treated LDL

ONOO⁻-treated LDL (Fig. 4A) displayed a decrease in optical rotativity at 200–260 nm for LDL⁻ as compared to nLDL. There was a distinctive difference in the CD spectra for LDL subfractions at 220 nm (LDL⁻ > tLDL > nLDL). As mentioned above, increasing optical rotativity at 220 nm reflects a loss in α -helical structure and an increase in β -sheet structure that was confirmed by CD deconvolution software (CDNN) assessing the percent structural integrity of the different LDL sub-fractions components of ONOO⁻-modified LDL (Fig. 4B). Interestingly, the percentage of structural components in *in vivo* LDL⁻ and that of ONOO⁻-treated LDL were similar (Fig. 4C).

SIN-1-modified LDL

Because atherosclerotic lesions have increased activities of iNOS/eNOS and NADPH oxidase, a flux of $\cdot\text{NO}$ and $\text{O}_2^{\cdot-}$ (to yield ONOO⁻) may be mimicked by SIN-1 and may further support findings by our laboratory showing increased nitration at bifurcations where oscillatory flow occurs and where atherosclerosis is prone to develop [15]. Nitrotyrosine- (Fig. 5A) and lipid peroxide (Fig. 5C) accumulation as well as the percentage of LDL⁻ formation (Fig. 5D) following incubation of LDL with SIN-1 were similar to those observed with ONOO⁻ (Fig. 3). SIN-1 also induced an oxidation of cysteine residues (Fig. 5B) greater than that obtained with ONOO⁻ (Fig. 3B).

Binding and uptake of ONOO⁻-modified LDL

The biological significance of modified LDL was assessed with respect to LDL binding to- (Fig. 6) and uptake by (Fig. 7) bovine aortic vascular endothelial (BAEC) cells. Binding experiments, performed at 0°C, are shown for DiI-labeled LDL (Fig. 6A) and DiI-labeled, ONOO⁻-treated LDL (Fig. 6B). Similar approaches with an excess of 200 $\mu\text{g}/\text{ml}$ unlabeled LDL were used to rule out DiI labeling of cell membranes and ascertain LDL binding specificity (Fig. 6C,D). Analysis of the mean fluorescence intensity indicated that binding of ONOO⁻-treated LDL was stronger than that of control LDL (Fig. 6E).

Uptake experiments, performed at 37°C, are shown in Fig. 7 with a similar approach to that in Fig. 6: DiI-labeled LDL (Fig. 7A) and DiI-labeled, ONOO⁻-treated LDL (Fig. 7B). As with binding experiments, uptake of ONOO⁻-treated LDL was slightly higher than that of native LDL (Fig. 7E). The stronger binding and uptake of ONOO⁻-treated LDL may suggest alternate uptake mechanisms as well as an increased uptake of unfolded proteins.

In the presence of a 20-fold excess of native LDL (Fig. 6C, Fig. 7C) or ONOO⁻-treated LDL (Fig. 6D, 7D), respectively, binding and uptake were significantly inhibited (Fig. 6E, Fig. 7E), thus suggesting that LDL is binding to- and taken up by cells rather than nonspecific labeling of BAEC plasma membranes with DiI.

Receptor-dependent binding and uptake of control- and ONOO⁻-LDL

Receptor-dependent binding (Fig. 8–9) and uptake (Fig. 10–11) of control- (Fig. 8, 10) and ONOO⁻-LDL (Fig. 9, 11) was determined by receptor blocking of LOX-1, CD36, SR-A and LDL-R with receptor blocking antibodies and by determining the amount of DiI-control-LDL and DiI-ONOO⁻-LDL mean binding and uptake intensities. Analysis of control-LDL showed that the majority of the control lipoprotein binding was initiated by LDL-R (Fig. 8E, G, $P < 0.01$); however there were minimal binding differences between all receptors blocked in the

presence of active LOX-1 (Fig. 8B, G), CD36 (Fig 8C, G), and SR-A (Fig. 8D, G). However, LDL-R was not completely involved in the binding of control-LDL since active LDL-R was unable to completely restore binding to no receptor blocking (Fig 8A, G). Incubating cells with excess unlabeled LDL was able to reduce the binding intensity of DiI-LDL suggesting that DiI was only minimally labeling the membranes and was not the majority of the labeling. These findings also demonstrate that control-LDL is bound to the non-atherogenic LDL-R with minimal binding from the three oxLDL-R, thus suggesting that the small amount of oxLDL *in vivo* may be binding to scavenger receptors *in vitro*.

ONOO⁻-modified LDL was significantly bound by LOX-1 (Fig. 9C, G, $P < 0.05$), CD36 (Fig. 9D, G, $P < 0.001$) and SR-A (Fig. 9E, G, $P < 0.01$) with SR-A and CD36 having the largest impact on binding whereas active LDL-R had no impact on LDL binding (Fig. 9F, G). These findings suggest that ONOO⁻-treated LDL is not binding through an aggregated LDL-R-dependent mechanism but rather by each of the three scavenger receptors (LOX-1, CD36, and SR-A).

Receptor-dependent uptake of control-LDL (Fig. 10) demonstrated that the particle is taken up significantly by LDL-R (Fig. 10F, G $P < 0.001$), whereas there is minimal involvement with LOX-1 (Fig. 10C, G), CD36 (Fig. 10D, G) and SR-A (Fig. 10E, G) scavenger receptors. These findings further support the motion that control-LDL has minimal modified LDL and is minimally atherogenic as compared to ONOO⁻-LDL.

The receptor-dependent uptake of ONOO⁻-treated LDL was significantly elevated for LOX-1 (Fig. 11C, G, $P < 0.05$), CD36 (Fig. 11D, G, $P < 0.01$), SR-A (Fig. 11E, G, $P < 0.001$), whereas LDL-R (Fig. 11F, G) was not significantly different from all receptors blocked suggesting that ONOO⁻-LDL is not internalized through an aggregated-LDL uptake mechanism. These findings further support the atherogenic character of ONOO⁻-treated LDL.

Discussion

LDL⁻ may be viewed as a circulating, atherogenic form of LDL *in vivo* and it harbors secondary structural changes in apoB-100 that encompass a significant loss of α -helical structure and increase in β -sheet structure [3]. This study addresses (a) the chemical modifications and structural changes inherent in LDL⁻ formation, (b) a functional role for ONOO⁻ in LDL⁻ formation, and (c) the occurrence of specific cellular receptors for LDL⁻.

Chemical modifications and structural changes in LDL⁻

LC/MS/MS (Table 1) and circular dichroism (Fig. 2) analyses indicated apoB-100 protein modifications and conformational changes inherent in LDL⁻. Although there were no observed nitrated peptides by LC/MS/MS in native- and total-LDL fractions *in vivo*, there was nitration that was quantified by LC/EIS/MS analysis. The amount of nitration observed for native LDL was 100 fold lower than LDL⁻ and tLDL was approximately 10–12 fold lower. These findings further support the notion that the LDL⁻ particle is the modified LDL subfraction *in vivo* as well as may support the LDL⁻ hypothesis. Tyrosine nitration in LDL⁻ (Table 1) in α_1 , α_2 , and α_3 helices as well as β_2 sheets as well as cysteine oxidation in β_1 to cysteic acid (Fig. 12) seem to assist the loss of α -helical structure in LDL⁻ and increase β -turn, parallel- and antiparallel sheets, and random coil structures (Fig. 2). Of note, nitration of apoB-100 occurs in the α -helical structures containing the highest percentage of tyrosine per total amino acid residues: α_1 appears to be more susceptible to nitrotyrosine formation, whereas β_1 seemed resistant to nitration and susceptible to cysteine oxidation. Nitration of α -helices appears to contribute to protein unfolding, whereas the oxidation of one of the nine free cysteines (in β_1 sheets) may be involved in the increased electronegativity of the particle.

A functional role for ONOO⁻ in LDL⁻ formation

Treatment of native LDL with either ONOO⁻ (Fig. 3) or SIN-1 (Fig. 5) resulted in extensive tyrosine nitration (Table 2; Fig. 12), accumulation of lipid peroxides, and loss of α -helical structure (Fig. 4) and, as a corollary, formation of LDL⁻ (Fig. 3D, Fig. 5D). It may be surmised, hence, that nitrotyrosine- and lipid peroxide accumulation are synergistically responsible for unfolding of α -helices inherent in LDL⁻ formation.

Specific cellular receptors for LDL⁻

The aforementioned protein modifications and structural changes in LDL⁻ may suggest an LDL receptor (LDL-R)-independent mechanism for binding and uptake of LDL⁻ to and into BAEC cells; this notion is supported by the following (a) LDL nitration coincides with the binding sites to LDL-R (encompassing amino acid residues 3359 and 3369 in β_2) and (b) there is evidence that ONOO⁻-treated LDL binds to CD36 [35]. These findings are further confirmed by the binding and uptake of ONOO⁻-treated LDL to LOX-1, CD36, and SR-A receptors in BAEC with minimal involvement of the non-atherogenic LDL-R. It is worth noting that most uptake and binding in control-LDL was dependent on LDL-R and independent of oxLDL-R suggesting the non atherogenic properties of control-LDL. However, there was still a minimal binding and uptake to LOX-1, CD36, and SR-A in control-LDL suggesting the importance of *in vivo* modified LDL⁻. It was also evident that ONOO⁻-treated LDL did not induce LDL-R mediated uptake suggesting that it is not being endocytosed through an aggregated-LDL uptake mechanism. The *in vivo* LDL⁻ nitration pattern and structure as well as ONOO⁻-modified LDL demonstrate that ONOO⁻ is the most likely mechanism of protein nitration *in vivo* and suggests that protein unfolded LDL induces scavenger receptor dependent binding and uptake and is further supported by enzymatic modifications that induce protein unfolding [3,17]. Nitrated LDL is also involved in an LDL-R independent binding and uptake mediated by SR-A, LOX-1, and CD36, thus strengthening the pathophysiological significance of ONOO⁻-driven LDL modifications, its unfolding, and the pathogenesis of atherosclerosis.

Tyrosine nitration and lipid peroxidation appear to disturb the phospholipid belt of LDL and hydrophobic stacking of aromatic amino acids in the lipid core. The three α -helices have the highest percentage of tyrosine residues; it may be hypothesized that nitration of these tyrosine residues would have a synergistic affect upon protein unfolding along with lipid peroxide formation. Addition of a nitro group to tyrosine involves the addition of a hydrophilic moiety with a net electrostatic charge (Zwitterion); aromatic groups are involved in hydrophobic stacking interactions in proteins as well as in protein-lipid bilayer interface. Therefore, nitration in α -helices is expected to interfere with hydrophobic stacking in the lipid core of the LDL particle and possibly with the phospholipid belts of α_2 and α_3 helices, leading to protein unfolding. Furthermore, peroxidation of lipids in LDL seem to cause unfolding of the apoB-100 protein [11]. The phospholipid belt in α_2 and α_3 is stabilized by electrostatic bonds between negatively charged phospho head groups and positively charged lysine/arginine residues. Peroxidation of long chain poly unsaturated fatty acyl chains of the phospholipid belts and the addition of molecular oxygen will increase the hydrophilicity of the fatty acyl chains of phospholipids, thus resulting in both the migration out of the lipid phase and an increasing surface area to volume ratio of the lipid core (increased hydrophilic surface). This increased strain would induce α_2 and α_3 to stretch and adopt a new confirmation. This mechanism strengthens the significance of the phospholipid belts (α_2 and α_3) in maintaining particle protein/lipid integrity, particle structure, proper electrostatic interactions, and aromatic stacking.

Regardless of its mechanism, these findings suggest that protein unfolding may be the main contributor to LDL⁻-induced atherosclerosis. The extensive nitration of apoB-100 in the α -helices and β -sheets of LDL⁻ and its absence in native LDL suggest that the latter is not or has

not been subjected to nitrate stress *in vivo*. In response to phospholipase A₂ and oxidation *in vitro*, modifications of LDL render the formation of an electronegative sub-fraction with secondary structural changes similar to those of *in vivo* LDL⁻. As an emergent marker for coronary artery disease, nitrotyrosine is prominent in atherosclerotic lesions as well as LDL isolated from atherosclerotic lesions [5]. In this context, this study established similar apoB-100 protein nitration patterns and secondary protein structural changes in *in vivo* circulating LDL⁻ and ONOO⁻-treated LDL. Moreover, binding and uptake of the protein unfolded fraction (LDL⁻) was higher than that of native LDL and uptake of ONOO⁻-treated LDL is dependent on scavenger receptors LOX-1, CD36, and SR-A and is not dependent on LDL-R whereas the control-LDL subfraction is dependent on anti-atherogenic LDL-R and not dependent on atherogenic LOX-1, CD36, and SR-A scavenger receptors in BAEC.

Supplementary Material

Refer to Web version on PubMed Central for supplementary material.

Abbreviations

LDL, low-density lipoprotein; nLDL, native LDL; tLDL, total LDL; LDL⁻, negatively-charged LDL, oxidatively-modified LDL; CD, circular dichroism; SIN-1, 3-morpholino-sydnonimine; DiI, 3,3,3',3'-tetramethylindocarbocyanine perchlorate; BAEC, bovine aortic endothelial cells; Apolipoprotein B-100, ApoB-100; LC/EIS/MS, Liquid Chromatography electron ion spray mass spectrometry.

Acknowledgements

We thank Dr. Ralf Langen and team for support with CD spectra analyses and CD spectrophotometer. We also thank Staley L. Hazen and team for their analysis of nitrotyrosine in ONOO⁻-treated LDL by LC/EIS/MS. This work was supported by AHA GIA 0655051Y (TKH), NIH HL 83015 (TKH), and HL NIH HL068689 (TKH). The authors would like to express gratitude to Dr. Alex Sevanian.

References

1. Colell A, Garcia-Ruiz C, Lluís JM, Coll O, Mari M, Fernandez-Checa JC. *J. Biol. Chem* 2003;278:33928–33935. [PubMed: 12821666]
2. Hevonoja T, Pentikainen MO, Hyvonen MT, Kovanen PT, Ala-Korpela M. *Biochim. Biophys. Acta* 2000;1488:189–210. [PubMed: 11082530]
3. Asatryan L, Hamilton RT, Isas JM, Hwang J, Kaye R, Sevanian A. *J. Lipid Res* 2005;46:115–122. [PubMed: 15489541]
4. Torzewski M, Lackner KJ. *Clin. Chem. Lab. Med* 2006;44:1389–1394. [PubMed: 17163812]
5. Leeuwenburgh C, Hardy MM, Hazen SL, Wagner P, Oh-ishi S, Steinbrecher UP, Heinecke JW. *J. Biol. Chem* 1997;272:1433–1436. [PubMed: 8999808]
6. Koller E, Volf I, Gurvitz A, Koller F. *Pathophysiol. Haemost. Thromb* 2006;35:322–345. [PubMed: 16877881]
7. Malle E, Marsche G, Arnhold J, Davies MJ. *Biochim. Biophys. Acta* 2006;1761:392–415. [PubMed: 16698314]
8. Osterud B, Bjorklid E. *Physiol. Rev* 2003;83:1069–1112. [PubMed: 14506301]
9. Gomes LF, Alves AF, Sevanian A, Peres Cde A, Cendoroglo MS, de Mello-Almada C, Quirino LM, Ramos LR, Junqueira VB. *Antioxid. Redox Signal* 2004;6:237–244. [PubMed: 15025925]
10. Hwang J, Rouhanizadeh M, Hamilton RT, Lin TC, Eiserich JP, Hodis HN, Hsiai TK. *Free Radic. Biol. Med* 2006;41:568–578. [PubMed: 16863990]
11. Ursini F, Davies KJ, Maiorino M, Parasassi T, Sevanian A. *Trends Mol. Med* 2002;8:370–374. [PubMed: 12127722]
12. Thomas SR, Davies MJ, Stocker R. *Chem. Res. Toxicol* 1998;11:484–494. [PubMed: 9585479]

13. Botti H, Batthyany C, Trostchansky A, Radi R, Freeman BA, Rubbo H. *Free Radic. Biol. Med* 2004;36:152–162. [PubMed: 14744627]
14. Hazen SL, Crowley JR, Mueller DM, Heinecke JW. *Free Radic. Biol. Med* 1997;23:909–916. [PubMed: 9378370]
15. Hsiai TK, Hwang J, Barr ML, Correa A, Hamilton R, Alavi M, Rouhanizadeh M, C E, Hazen SL. *Free Radic. Biol. Med* 2007;42:519–529. [PubMed: 17275684]
16. Han SR, Momeni A, Strach K, Suriyaphol P, Fenske D, Paprotka K, Hashimoto SI, Torzewski M, Bhadki S, Husmann M. *Atheros. Thromb. Vasc. Biol* 2003;23:661–667.
17. Dersch K, Ichijo H, Bhadki S, Husmann M. *Cell Death Differ* 2005;12:1107–1114. [PubMed: 15846374]
18. Torzewski M, Suriyaphol P, Paprotka K, Spath L, Ochsenhirt V, Schmitt A, Han SR, Husman M, Gerl VB, Bhadki S, Lackner KJ. *Atheros. Thromb. Vasc. Biol* 2004;24:2130–2136.
19. Saad AF, Virella G, Chassereau C, Boackle RJ, Lopes-Virella MF. *J. Lipid Res* 2006;47:1975–1983. [PubMed: 16804192]
20. Hsiai TK, Cho SK, Wong PK, Ing M, Salazar A, Sevanian A, Navab M, Demer LL, Ho CM. *Faseb J* 2003;17:1648–1657. [PubMed: 12958171]
21. Jagavelu K, Tietge UJ, Gastel M, Drexler H, Schieffer B, Bavendiek U. *Circ. Res.* 2007in press
22. Zheng L, Nukuna B, Brennan ML, Sun M, Goormastic M, Settle M, Schmitt D, Fu X, Thomson L, Fox PL, Ischiropoulos H, Smith JD, Kinter M, Hazen SL. *J. Clin. Invest* 2004;114:529–541. [PubMed: 15314690]
23. Ferraro B, Galli F, Frei B, Kingdon E, Canestrari F, Rice-Evans C, Buoncristiani U, Davenport A, Moore KP. *Kidney Int* 2003;63:2207–2213. [PubMed: 12753309]
24. Yamaguchi Y, Matsuno S, Kagota S, Haginaka J, Kunitomo M. *Atherosclerosis* 2004;172:259–265. [PubMed: 15019535]
25. Spite M, Baba SP, YAhmed Y, Barski OA, Nijhawan K, Petrash JM, Bahatnagar A, Srivastava S. *Biochem. J* 2007;405:95–105. [PubMed: 17381426]
26. Hwang J, Wang J, Morazzoni P, Hodis HN, Sevanian A. *Free Radic. Biol. Med* 2003;34:1271–1282. [PubMed: 12726915]
27. Stocker R, Keaney JF Jr. *J. Thromb. Haemost* 2005;3:1825–1834. [PubMed: 16102049]
28. Behr-Roussel D, Rupin A, Simonet S, Bonhomme E, Coumilleau S, Cordi A, Serkiz B, Fabiani JN, Verbeuren TJ. *Circulation* 2000;102:1033–1038. [PubMed: 10961969]
29. Hodis HN, Kramsch DM, Avogaro P, Bittolo-Bon G, Cazzolato G, Hwang J, Peterson H, Sevanian A. *J. Lipid Res* 1994;35:669–677. [PubMed: 8006522]
30. Feelisch M, Ostrowski J, Noack E. *J. Cardiovasc. Pharmacol* 1989;14:S13–S22. [PubMed: 2484692]
31. Ducret A, Van Oostveen I, Eng JK, Yates Jr, Aebersold R. *Protein Sci* 1998;7:706–719. [PubMed: 9541403]
32. Perkins DN, Pappin DJC, Creasy DM, Cottrell JS. *Electrophoresis* 1999;20:3551–3567. [PubMed: 10612281]
33. Ricci R, Sumara G, Sumara I, Rozenberg I, Kurrer M, Akhmedov A, Hersberger M, Eriksson U, Eberli FR, Becher B, Boren J, Chen M, Cybulsky MI, Moore KJ, Freeman MW, Wagner EF, Matter CM, Luscher TF. *Science* 2004;306:1558–1561. [PubMed: 15567863]
34. Sevanian A, Bittolo-Bon G, Cazzolato G, Hodis H, Hwang J, Zamburlini A, Maiorino M, Ursini F. *J Lipid Res* 1997;38:419–428. [PubMed: 9101423]
35. Guy RA, Maguire GF, Crandall I, Connelly PW, Kain KC. *Atherosclerosis* 2001;155:19–28. [PubMed: 11223422]

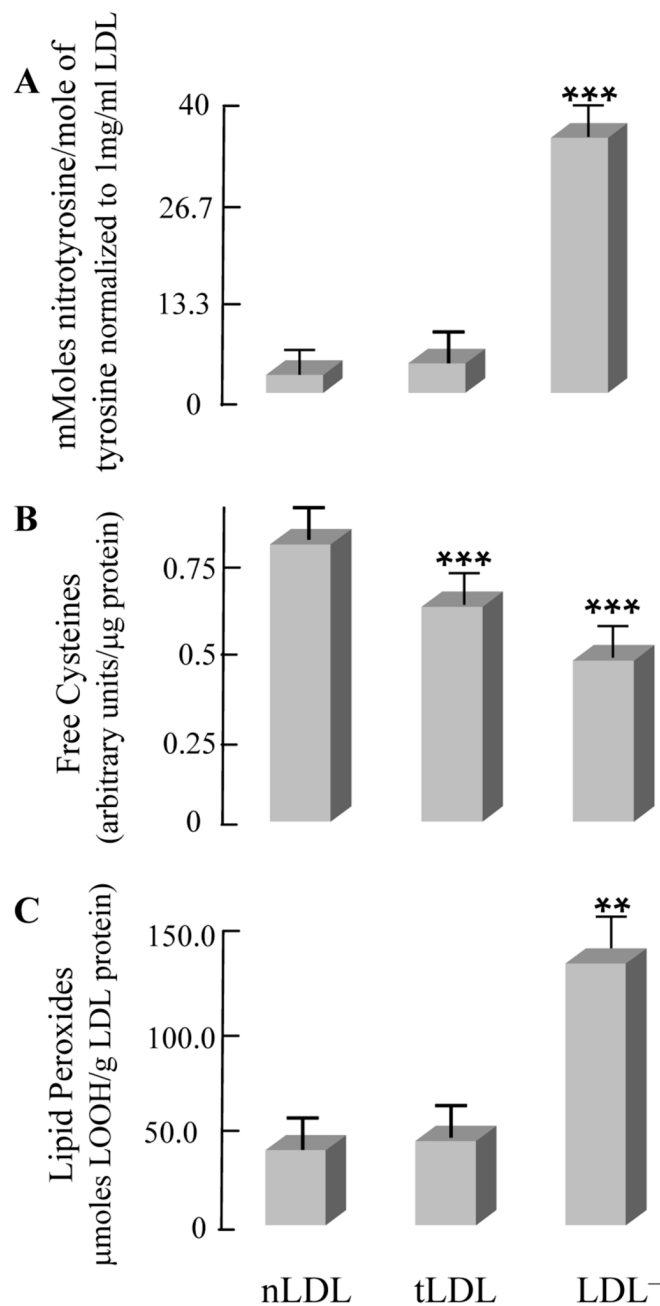


Fig. 1. Chemical modifications of in vivo LDL subfractions

LDL sub-fractions were isolated by anion exchange chromatography as described in the Materials and Methods section and analyzed for (A) Nitrotyrosine content, (B) Free cysteine content (biotin labeling), and labeling, and (C) Lipid peroxide content. ($n = 3$, $*P < 0.05$, $**P < 0.01$; $***P < 0.001$).

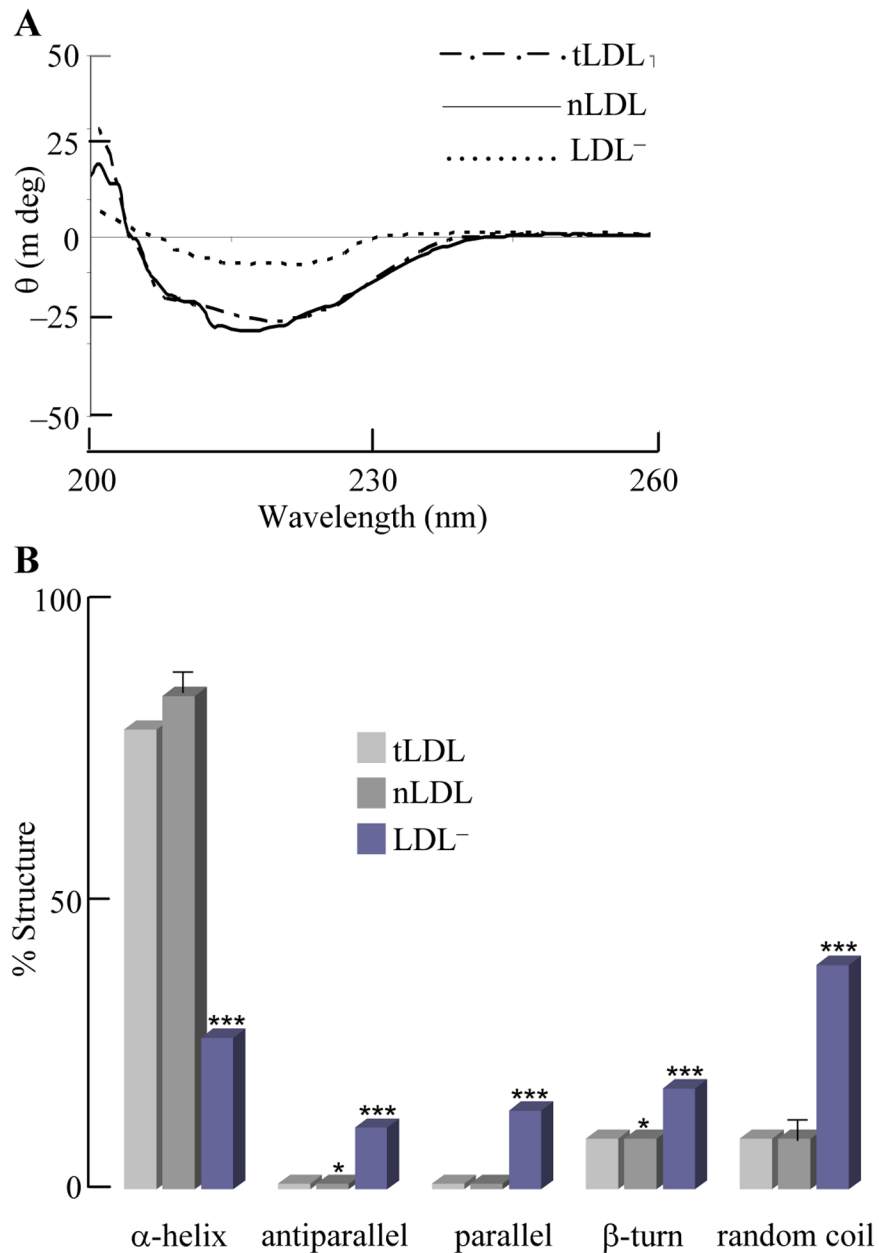


Fig. 2. Circular dichroism spectral analyses of in vivo LDL subfractions

(A) Circular dichroism spectra for different LDL subfractions were performed as described in the Materials and Methods section. (B) Secondary structures of LDL subfractions; data were obtained from spectra in (A), which were deconvoluted for apoB-100 secondary structure. ($n = 3$, * $P < 0.05$, ** $P < 0.01$, *** $P < 0.001$).

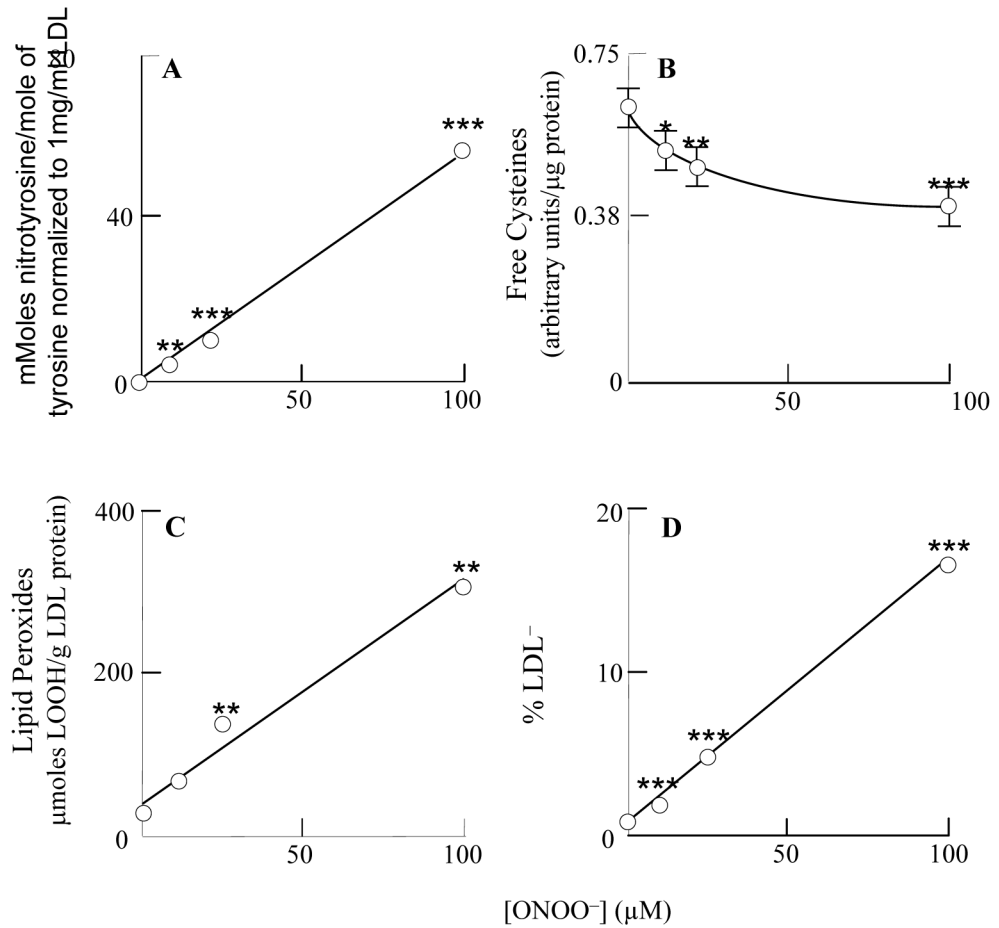


Fig. 3. ONOO⁻-modified LDL

LDL samples were supplemented with different amounts of ONOO⁻ and analyzed for (A) nitrotyrosine, (B) free cysteine (after biotin labeling), (C), lipid peroxides, and LDL⁻ content (percentage). ($n = 3$, $*P < 0.05$, $**P < 0.01$; $***P < 0.001$).

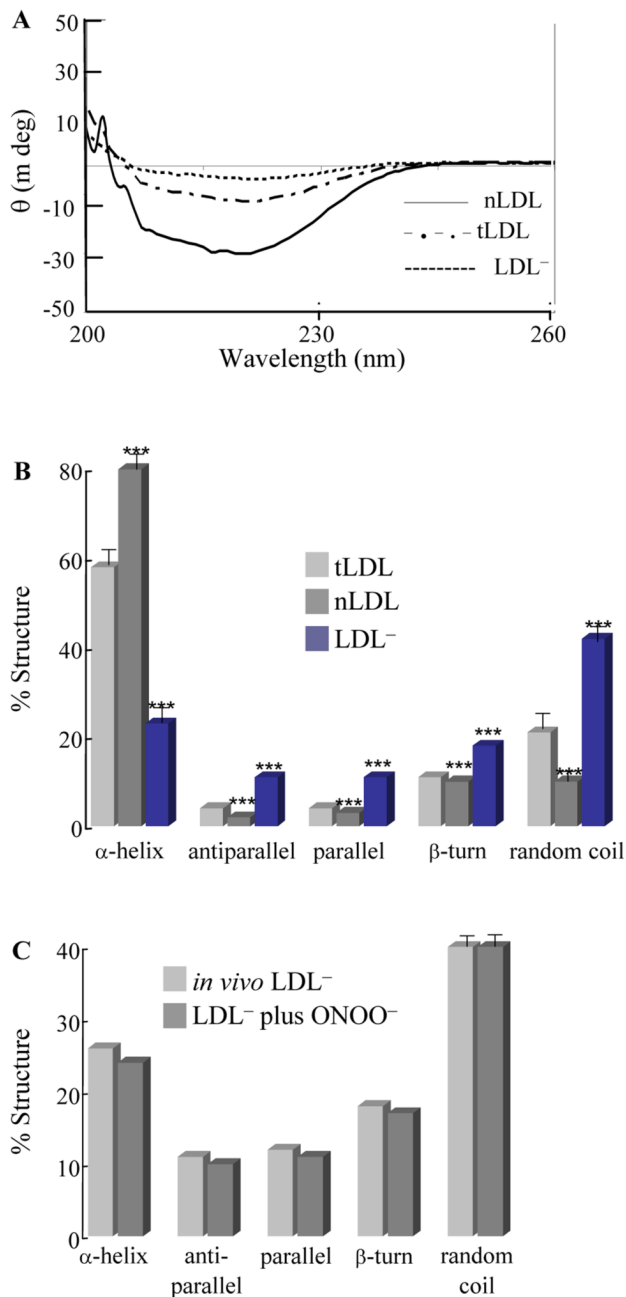


Fig. 4. Circular dichroism spectral analyses of ONOO⁻-modified LDL (tLDL was treated with 10 μM ONOO⁻ as described in the Materials and Methods section); the ONOO⁻-treated tLDL was fractionated into nLDL and LDL⁻ components and CD spectra were determined. (A) Circular dichroism spectra of LDL subfractions. (B) Secondary structure of different LDL subfractions. CD deconvolution software was used to determine the changes in the structures of the LDL sub-fractions. (C) Comparison of secondary structure components in *in vivo* LDL⁻ and LDL⁻ from ONOO⁻-treated tLDL. Data taken from Fig. 2B (for *in vivo* LDL⁻) and Fig. 4B (LDL⁻ fraction of the ONOO⁻-treated tLDL). ($n = 3$, $*P < 0.05$, $**P < 0.01$; $***P < 0.001$).

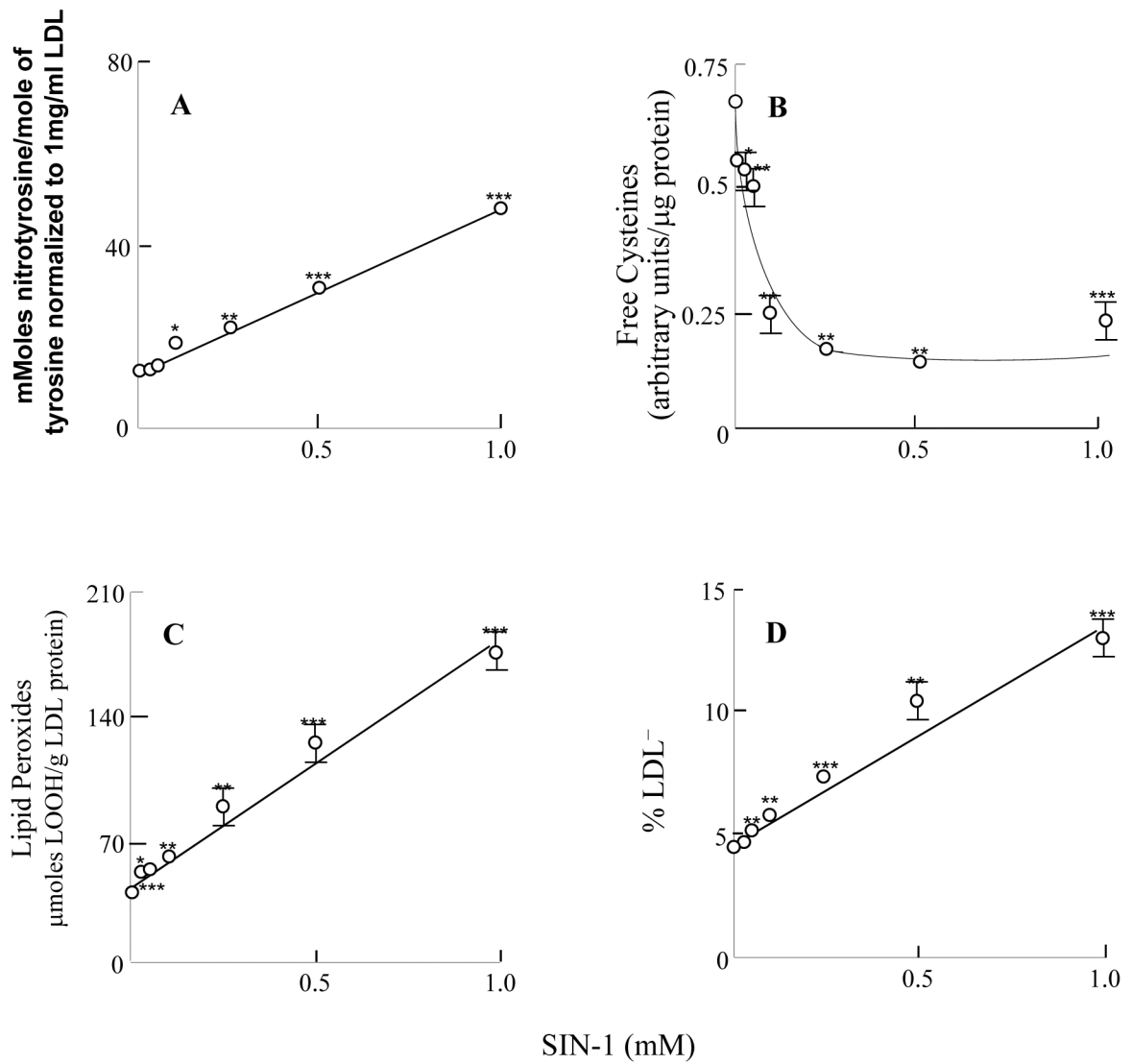


Fig. 5. SIN-1-modified LDL

LDL particles were incubated with different amounts of SIN-1 and analyzed for (A) nitrotyrosine, (B) free cysteine, (C) lipid peroxides, and (D) percentage of LDL⁻ as described in the Materials and Methods section. ($n = 3$, * $P < 0.05$, ** $P < 0.01$; *** $P < 0.001$).

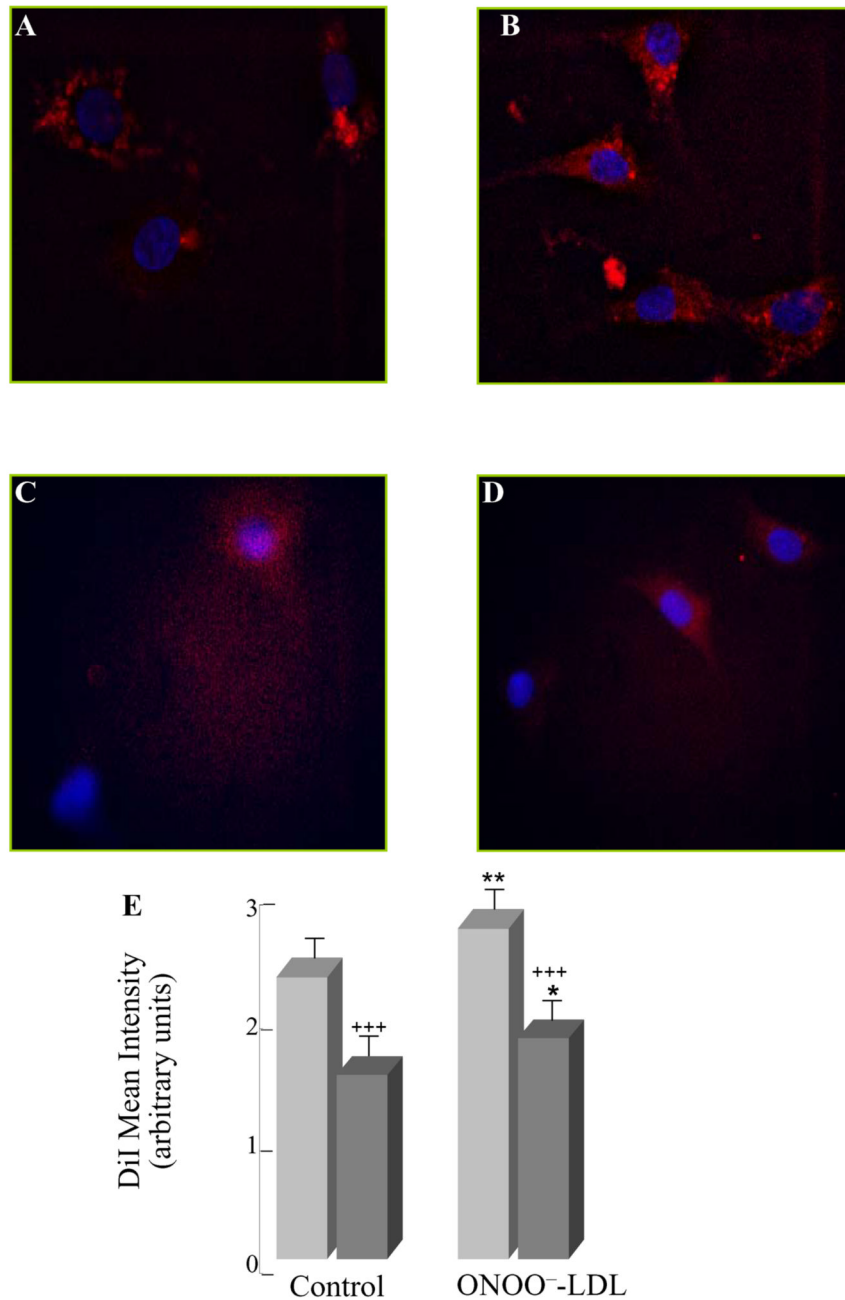


Fig. 6. Binding of ONOO⁻-modified LDL

LDL binding experiments were performed at 0°C for 90 min with the following conditions: (A) control-LDL 10 μg/ml DiI-LDL, (B) ONOO⁻-treated LDL 10 μg/ml DiI-PN-LDL, (C) control-LDL 10 μg/ml DiI-LDL + 200 μg/ml unlabeled control-LDL, and (D) ONOO⁻-treated LDL 10 μg/ml DiI-PN-LDL + excess unlabeled ONOO⁻-treated LDL 200 μg/ml. Binding mean intensity of DiI labeled LDL was quantified using Axiom 200M Zeiss Fluorescent Microscope (E). Experiments were performed in triplicate and statistical significance to control-LDL and to the excess unlabeled LDL ($P < 0.01$) was determined. ($n = 3$, +, * $P < 0.05$, ++, ** $P < 0.01$; +++, *** $P < 0.001$).

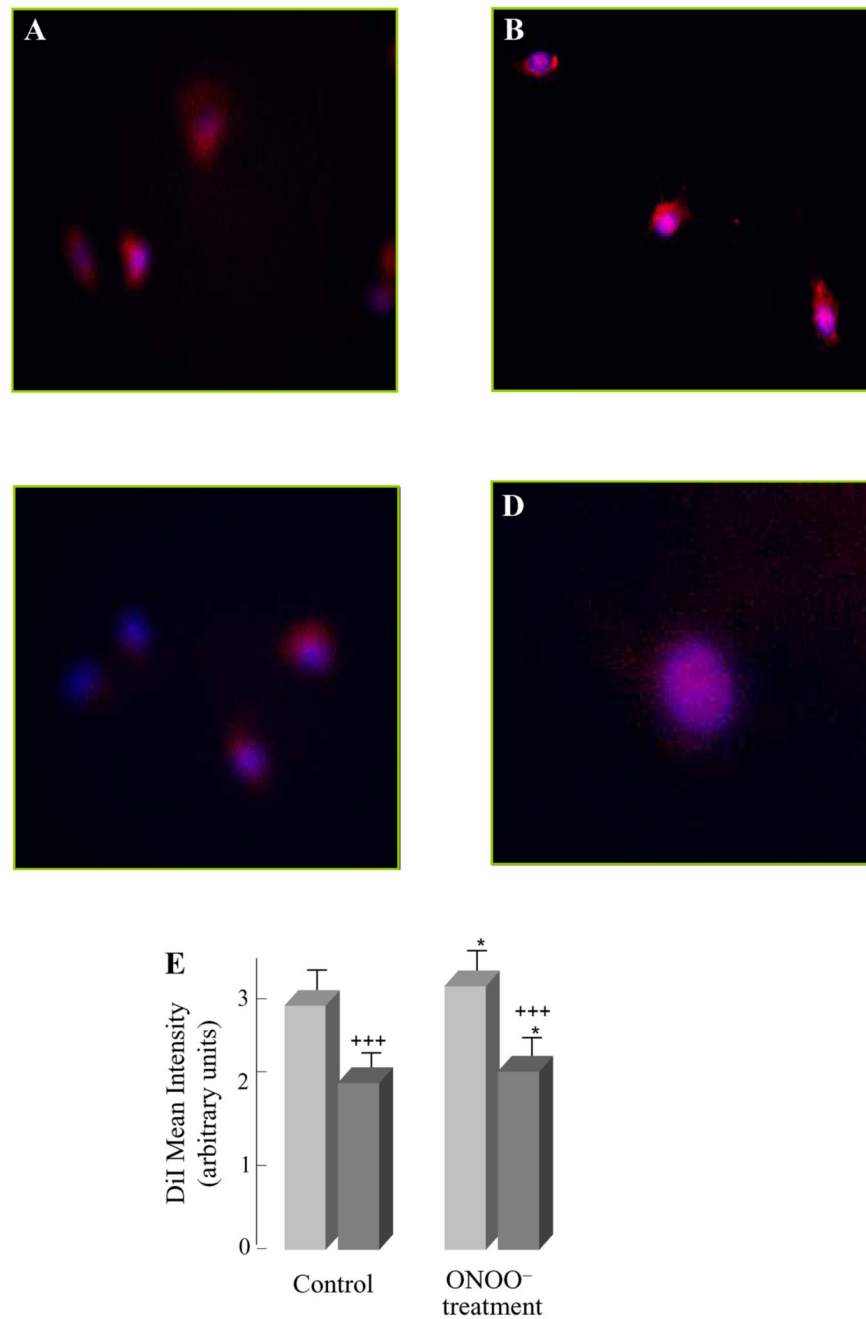


Fig. 7. Uptake of ONOO⁻-modified LDL

LDL uptake experiments were performed at 37°C for 4 h with the following conditions; (A) control-LDL 10µg/ml DiI-LDL, (B) ONOO⁻-treated LDL 10µg/ml DiI-PN-LDL, (C) control-LDL 10µg/ml DiI-LDL + 200µg/ml unlabeled control-LDL, and (D) ONOO⁻-treated LDL 10µg/ml DiI-PN-LDL + excess unlabeled ONOO⁻-treated LDL 200µg/ml (D). Uptake mean intensity of DiI labeled LDL was quantified using Axiom 200M Zeiss Fluorescent Microscope (E). Experiments were performed in triplicate and statistical significance to control-LDL ($P < 0.001$) and to the excess unlabeled LDL ($P < 0.001$) was determined. ($n = 3$, *, * $P < 0.05$, **, ** $P < 0.01$; ***, *** $P < 0.001$).

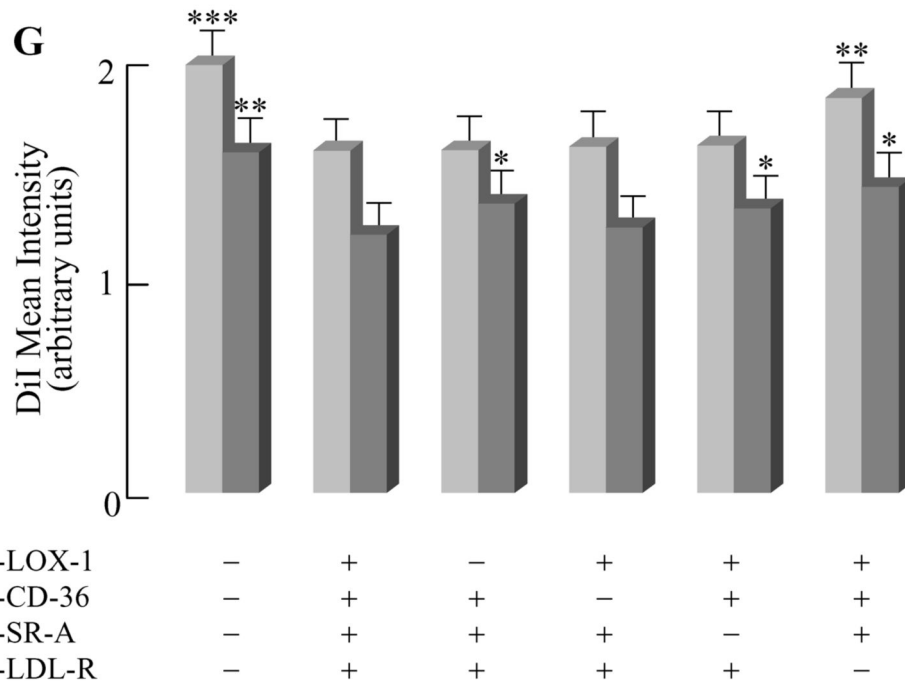
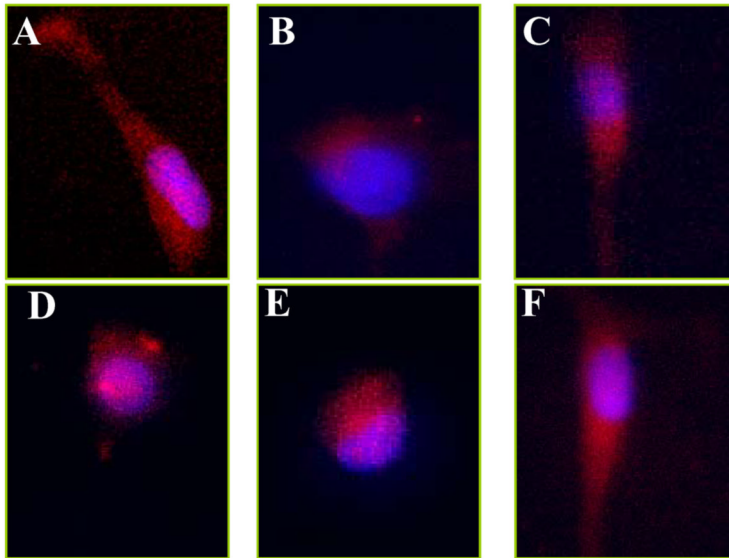


Fig. 8. Binding of control-LDL after receptor blocking

LDL receptor blocking was performed for 1 hour at 37°C and binding was determined at 0°C with 10 µg/ml DiI-control-LDL and 10 µg/ml DiI-control-LDL with 200 µg/ml excess unlabeled LDL for 90 minutes by the following conditions; (A) no receptor blocking with 10µg/ml DiI-control-LDL, (B) all four receptor's blocked with 10 µg/ml DiI-control-LDL (C) active LOX-1, (D) active CD36 with 10 µg/ml DiI-control-LDL, (E) active SR-A with 10 µg/ml DiI-control-LDL, and (F) active LDL-R with 10µg/ml DiI-control-LDL. Binding mean intensity of DiI-control-LDL was quantified using Axiom 200M Zeiss Fluorescent Microscope (G). Images are not shown for excess unlabeled control-LDL but intensities were quantified. Experiments were performed in triplicate and statistical significance was determined to all

receptors blocked to determine receptors significantly involved in the binding of DiI-labeled control-LDL (n=3, *-P<0.05, **-P<0.01, ***P<0.001). ■ - 10 mg/ml DiI-labeled control-LDL
■ - 10 mg/ml DiI-labeled control-LDL + 200 mg/ml excess unlabeled control-LDL.

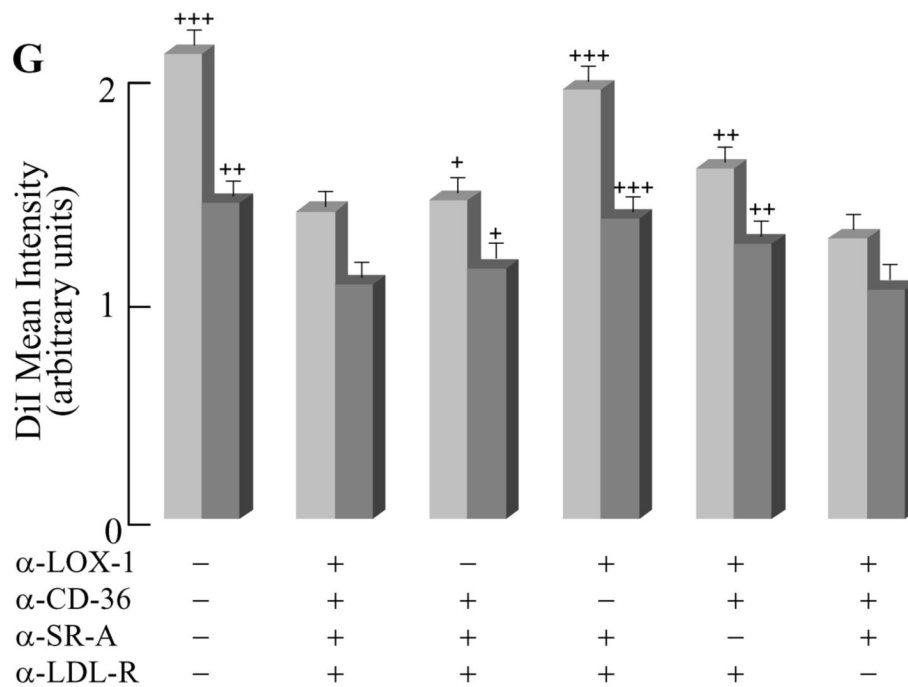
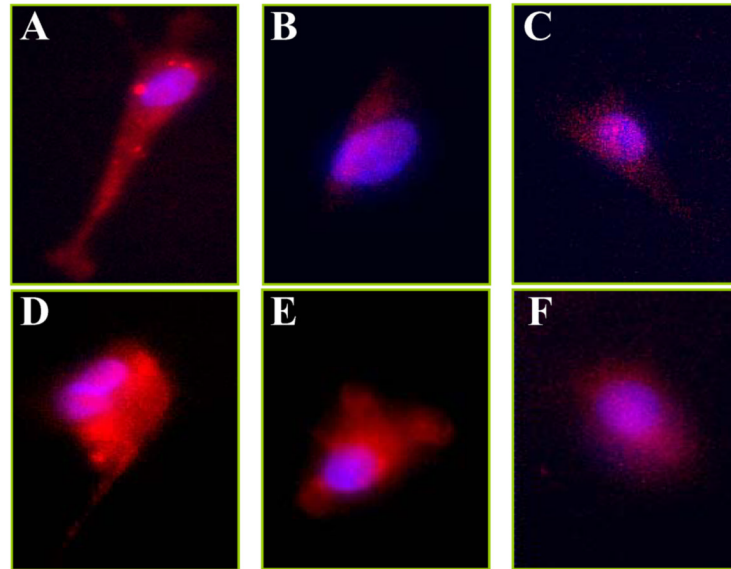


Fig. 9. Binding of ONOO⁻-LDL after receptor blocking

LDL receptor blocking was performed for 1 hour at 37°C and binding was determined at 0°C with 10µg/ml DiI-ONOO⁻-LDL and 10 µg/ml DiI-ONOO⁻-LDL with 200µg/ml excess unlabeled LDL for 90 minutes by the following conditions; (A) no receptor blocking with 10µg/ml DiI-ONOO⁻-treated LDL, (B) all four receptor's blocked with 10 µg/ml DiI-ONOO⁻-treated LDL (C) active LOX-1, (D) active CD36 with 10µg/ml DiI-ONOO⁻-treated LDL, (E) active SR-A with 10µg/ml DiI-ONOO⁻-treated LDL, and (F) active LDL-R with 10µg/ml DiI-ONOO⁻-treated LDL. Binding mean intensity of DiI-ONOO⁻-treated LDL was quantified using Axiom 200M Zeiss Fluorescent Microscope (G). Images are not shown for excess unlabeled ONOO⁻-treated LDL but intensities were quantified. Experiments were

performed in triplicate and statistical significance was determined to all receptors blocked to determine receptors significantly involved in the binding of DiI-labeled ONOO⁻-LDL (n=3, *-P<0.05, **-P<0.01, ***P<0.001). ■- 10 mg/ml DiI-labeled ONOO⁻-treated LDL, ■- 10 mg/ml DiI-labeled ONOO⁻-treated LDL + 200 mg/ml excess unlabeled ONOO⁻-treated LDL.

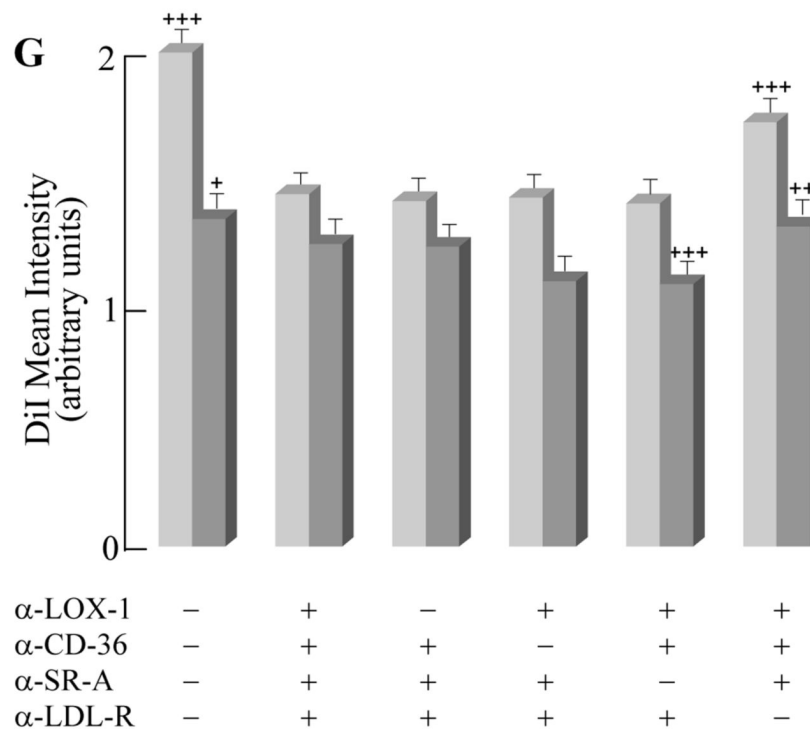
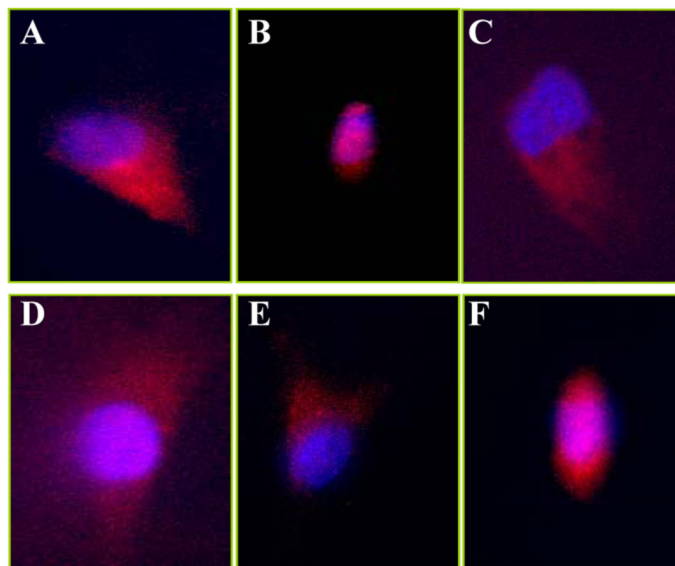


Fig. 10. Uptake of control-LDL after receptor blocking

LDL receptor blocking was performed for 1 hour at 37°C and uptake was determined at 37°C with 10 μ g/ml DiI-control-LDL and 10 μ g/ml DiI-control-LDL with 200 μ g/ml excess unlabeled LDL for 4 hours by the following conditions; (A) no receptor blocking with 10 μ g/ml DiI-control-LDL, (B) all four receptor's blocked with 10 μ g/ml DiI-control-LDL (C) active LOX-1, (D) active CD36 with 10 μ g/ml DiI-control-LDL, (E) active SR-A with 10 μ g/ml DiI-control-LDL, and (F) active LDL-R with 10 μ g/ml DiI-control-LDL. Uptake mean intensity of DiI-control-LDL was quantified using Axiom 200M Zeiss Fluorescent Microscope (G). Images are not shown for excess unlabeled control-LDL but intensities were quantified. Experiments were performed in triplicate and statistical significance was determined to all receptors blocked

to determine receptors significantly involved in the uptake of DiI-labeled control-LDL (n=3, *-P<0.05, **-P<0.01, ***P<0.001). ■- 10 mg/ml DiI-labeled control-LDL, ■- 10 mg/ml DiI-labeled control-LDL + 200 mg/ml excess unlabeled control-LDL.

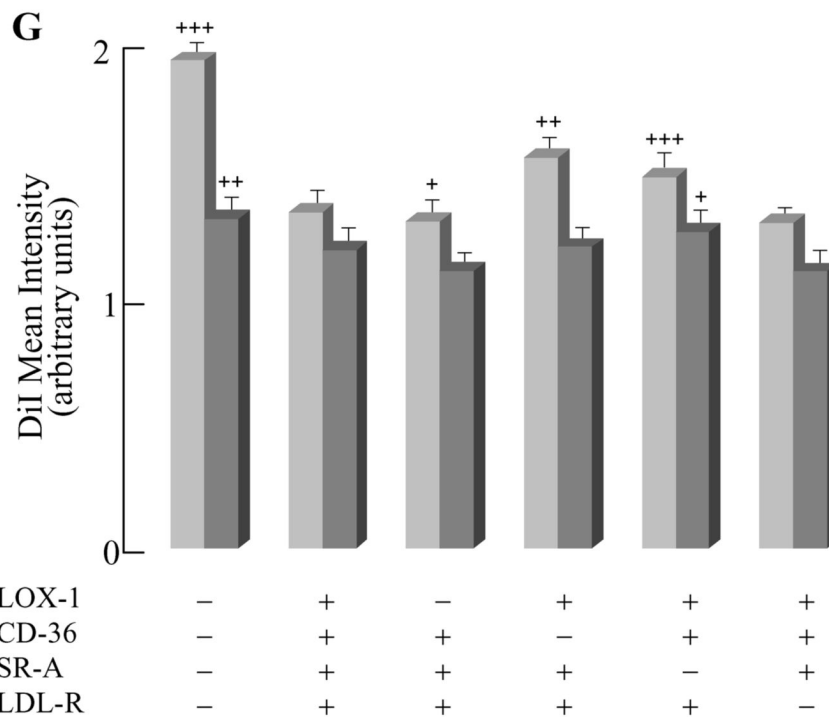
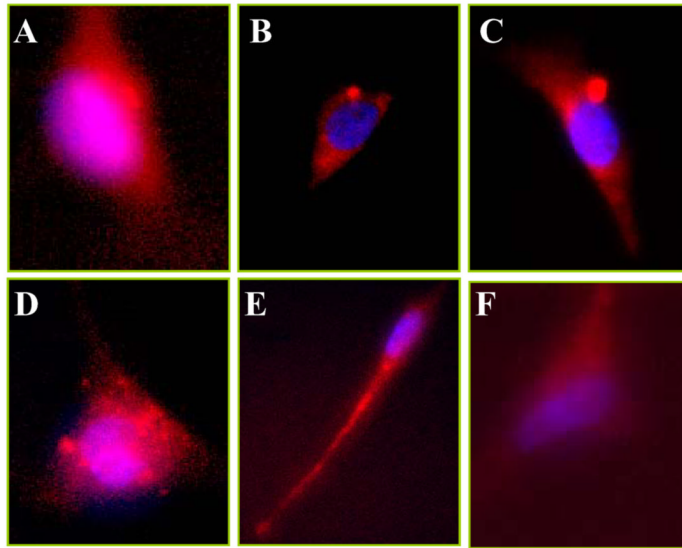


Fig. 11. Uptake of ONOO⁻-LDL after receptor blocking

LDL receptor blocking was performed for 1 hour at 37°C and uptake was determined at 0°C with 10 μ g/ml DiI-ONOO⁻-LDL and 10 μ g/ml DiI-ONOO⁻-treated LDL with 200 μ g/ml excess unlabeled ONOO⁻-treated LDL for 4 hours by the following conditions; (A) no receptor blocking with 10 μ g/ml DiI-ONOO⁻-treated LDL, (B) all four receptor's blocked with 10 μ g/ml DiI-ONOO⁻-treated LDL (C) active LOX-1, (D) active CD36 with 10 μ g/ml DiI-ONOO⁻-treated LDL, (E) active SR-A with 10 μ g/ml DiI-ONOO⁻-treated LDL, and (F) active LDL-R with 10 μ g/ml DiI-ONOO⁻-treated LDL. Binding mean intensity of DiI-ONOO⁻-treated LDL was quantified using Axiom 200M Zeiss Fluorescent Microscope (G). Images are not shown for excess unlabeled ONOO⁻-treated LDL but intensities were quantified. Experiments were

performed in triplicate and statistical significance was determined to all receptors blocked to determine receptors significantly involved in the binding of DiI-labeled ONOO⁻-treated LDL. Experiments were performed in triplicate and statistical significance was determined to all receptors blocked (n=3, *-P<0.05, **-P<0.01, ***P<0.001). ■- 10 mg/ml DiI-labeled ONOO⁻-treated LDL, ■- 10 mg/ml DiI-labeled ONOO⁻-treated LDL + 200 mg/ml excess unlabeled ONOO⁻-treated LDL.

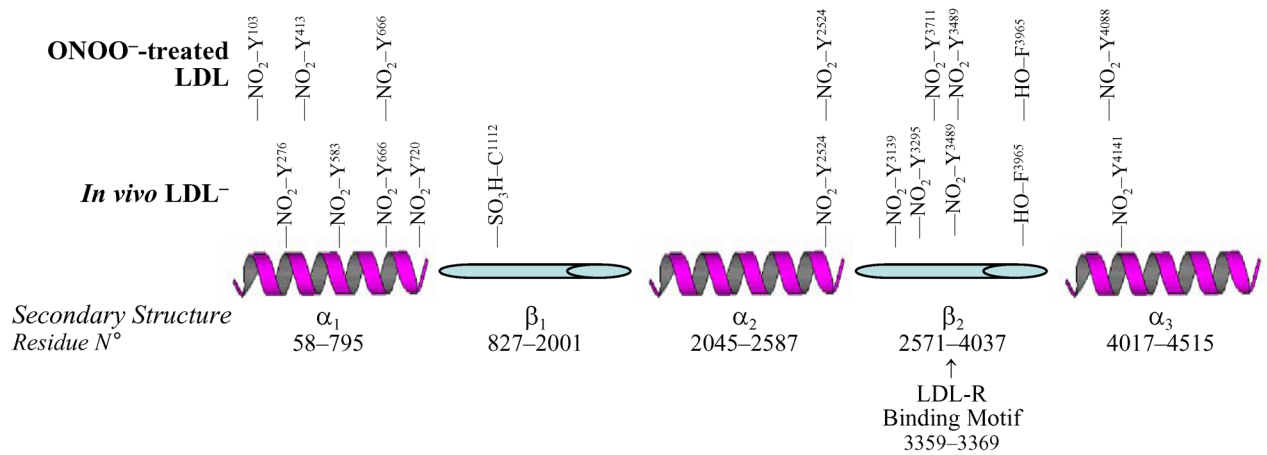


Fig. 12. Site of chemical modifications in *in vivo* LDL⁻ and ONOO⁻-treated LDL

The secondary structure of the apoB-100 is shown. The pentapartite structure however is not drawn to scale. Data from Table 1 and Table 2 were used to assign the chemical modifications in LDL⁻ and ONOO⁻-treated LDL.

Table 1
LC/MS/MS analyses of LDL⁻ Apo-B100 protein modifications

Secondary Structure	Peptide	Modified AA	sequence	MSc	charge	XC	Acn	modification	% modified
α_1	276-287	NO ₂ -Tyr ²⁷⁶	Y*GMVAQVTQTLLK	51	2	2.8	0.4	nitrotyrosine	100 ± 0
α_1	580-589	NO ₂ -Trp ⁵⁸³	IVQILPW*EQNEQV	30	2	3.0	0.2	nitrotryptophan	49.8 ± 0.6
α_1	580-589	HO-Trp ⁵⁸³	IVQILPW*EQNEQV	38	2	3.8	0.3	hydroxytryptophan	32.6 ± 1.9
α_1	655-669	NO ₂ -Tyr ⁶⁶⁶	IEGNLIFDPNNY*LPK	46	2	3.3	0.4	nitrotyrosine	18.3 ± 0.7
α_1	718-732	NO ₂ -Tyr ⁷²⁰	ALY*WAVNGQVPDGVSK	49	2	2.4	0.1	nitrotyrosine	29.9 ± 0.07
β_1	1101-1115	SO ₃ H-Cys ¹¹¹²	ITEVALMGHLSC*DTK	84	2	4.9	0.5	cysteic acid	100 ± 0
α_2	2523-2534	NO ₂ -Tyr ²⁵²⁴	MY*QMDIQEQLQR	36	2	3.0	0.3	nitrotyrosine	87.1 ± 0.2
β_2	3137-3148	NO ₂ -Tyr ³¹³⁹	LPY*TIITPPLK	30	2	1.9	0.5	nitrotyrosine	60.2 ± 0.2
β_2	3292-3311	NO ₂ -Tyr ³²⁹⁵	VPSY*TLILPSLELPLHLVPR	70	2	5.6	0.5	nitrotyrosine	80.4 ± 0.2
β_2	3481-3497	NO ₂ -Tyr ³⁴⁸⁹	LSLESLSY*FSIESSTK	62	2	4.7	0.7	nitrotyrosine	27.1 ± 1.1
β_2	3953-3973	HO-Phe ³⁹⁶⁵	DFSAEYEEDGKF*EGLQEWEGK	59	2	2.5	0.5	HO-phenylalanine	92.6 ± 0.9
α_3	4133-4145	NO ₂ -Tyr ⁴¹⁴¹	AASGTTGT*QEWK	46	2	2.7	0.1	nitrotyrosine	81.8 ± 0.1

Quantification of NO₂-Y
mMoles NO₂-Y/(mMoles Y)
LDL⁻ = 34.8 ± 1.0
tLDL = 2.0 ± 0.2
nLDL = 0.3 ± 0.1

* Full annotated MS spectra are represented in the order presented in this table in figures 1-12 of the supplemental section

Table 2

LC/MS/MS analyses of ONOO⁻-modified LDL Apo-B100

Secondary Structure	Peptide	Modified AA	sequence	MSc	charge	XC	Acn	modification	% modified
α_1	101–110	NO ₂ -Tyr ¹⁰³	Evy *gfnpegk	29	1	1.7	0.4	nitrotyrosine	49.9±1.7
α_1	401–427	NO ₂ -Tyr ⁴¹³	Vhanplidwty *lvalipepsaqqlr	33	2	2.6	0.3	nitrotyrosine	53.7±1.4
α_1	655–669	NO ₂ -Tyr ⁶⁶⁶	Iegnlifdpnny *lpk	28	2	2.8	0.4	nitrotyrosine	81.5±3.3
α_2	2523–2534	NO ₂ -Tyr ²⁵²⁴	My *qndiqqlqr	65	2	3.7	0.4	nitrotyrosine	66.6±5.9
β_2	3481–3497	NO ₂ -Tyr ³⁴⁸⁹	Islesltsy *fsiesstik	20	2	0.2	2.0	nitrotyrosine	41.3±0.6
β_2	3767–3772	NO ₂ -Tyr ³⁷⁷¹	eiqiy *k	25	1	0.1	1.3	nitrotyrosine	29.1±0.7
β_2	3953–3973	HO-Phe ³⁹⁶⁵	dfsaeeyedgkfcglqewegk	30	2	3.7	0.4	HO-phenylalanine	86.3±0.2
α_3	4088–4098	NO ₂ -Tyr ⁴⁰⁸⁸	Y *hwehtgltr	28	2	2.1	0.3	nitrotyrosine	95.3±0.8

Quantification of NO₂-Y
mMoles NO₂-Y/(moles Y)
54.2 ± 1.3

* Full annotated MS spectra are represented in the order presented in this table in figures 13–20 of the supplemental section